Neurosci. Bull. April, 2019, 35(2):183–192
https://doi.org/10.1007/s12264-018-0300-0

www.neurosci.cn
www.springer.com/12264

ORIGINAL ARTICLE

Phosphorylated TDP-43 Staging of Primary Age-Related Tauopathy

Xiaoling Zhang[1] · Bing Sun[1] · Xing Wang[2] · Hui Lu[1] · Fangjie Shao[2] · Annemieke J. M. Rozemuller[3] · Huazheng Liang[4] · Chong Liu[1,2] · Jiadong Chen[1] · Manli Huang[5] · Keqing Zhu[1,2]

Received: 4 April 2018 / Accepted: 1 August 2018 / Published online: 31 October 2018

Abstract Primary age-related tauopathy (PART) is characterized by tau neurofibrillary tangles (NFTs) in the absence of amyloid plaque pathology. In the present study, we analyzed the distribution patterns of phosphorylated 43-kDa TAR DNA-binding protein (pTDP-43) in the brains of patients with PART. Immunohistochemistry and immunofluorescence double-labeling in multiple brain regions was performed on brain tissues from PART, Alzheimer's disease (AD), and aging control cases. We examined the regional distribution patterns of pTDP-43 intraneuronal inclusions in PART with Braak NFT stages > 0 and $\leq$ IV, and a Thal phase of 0 (no beta-amyloid present). We found four stages which indicated potentially sequential dissemination of pTDP-43 in PART. Stage I was characterized by the presence of pTDP-43 lesions in the amygdala, stage II by such lesions in the hippocampus, stage III by spread of pTDP-43 to the neocortex, and stage IV by pTDP-43 lesions in the putamen, pallidum, and insular cortex. In general, the distribution pattern of pTDP-43 pathology in PART cases was similar to the early TDP-43 stages reported in AD, but tended to be more restricted to the limbic system. However, there were some differences in the distribution patterns of pTDP-43 between PART and AD, especially in the dentate gyrus of the hippocampus. Positive correlations were found in PART between the Braak NFT stage and the pTDP-43 stage and density.

Keywords TDP-43 · Primary age-related tauopathy · Alzheimer's disease · Neurofibrillary tangle · Hippocampus

Xiaoling Zhang, Bing Sun and Xing Wang contributed equally to this work.

Electronic supplementary material The online version of this article (https://doi.org/10.1007/s12264-018-0300-0) contains supplementary material, which is available to authorized users.

✉ Keqing Zhu
zhukeqing@zju.edu.cn

[1] China Brain Bank and Department of Neurology in Second Affiliated Hospital, Key Laboratory of Medical Neurobiology of Zhejiang Province, Department of Neurobiology, Zhejiang University School of Medicine, Hangzhou 310058, China

[2] Department of Pathology, Zhejiang University School of Medicine, Hangzhou 310058, China

[3] Department of Pathology, Amsterdam Neuroscience, VU University Medical Center, P.O. Box 7057, 1007 MB Amsterdam, The Netherlands

[4] Brain Structure and Function Group, Neuroscience Research Australia, Randwick, NSW 2031, Australia

[5] Department of Psychiatry, First Affiliated Hospital, Zhejiang University School of Medicine, Hangzhou 310003, China

Introduction

Primary age-related tauopathy (PART) is defined by the presence of Alzheimer's disease (AD)-type neurofibrillary changes without, or with few amyloid beta (Aβ) plaques. PART can be designated "Definite" or "Possible" depending on the presence of Aβ plaques. The working classification for definite PART is based on the presence of neurofibrillary tangles (NFTs) along with Braak stage $\leq$ IV and Thal Aβ Phase 0 [1]. Based on the working neuropathological diagnostic criteria, we have found that PART is common in the Chinese population as observed in specimens from our newly-established brain bank. But it is still not clear whether PART is a subtype of AD or a distinct tauopathy different from AD [2, 3]. PART, a new nomenclature, raises awareness of this common

pathological change and provides a conceptual foundation for further studies.

TAR DNA-binding protein of 43 kDa (TDP-43) is a major component that characterizes the most common pathological subtype of frontotemporal lobar degeneration (FTLD-TDP) and amyotrophic lateral sclerosis (ALS) [4–6]. Recently, immunohistochemical examination has demonstrated abnormal intracellular accumulation of TDP-43 in neurodegenerative disorders other than FTLD-TDP and ALS. These include AD (20%–50%), Parkinson's disease (7%), Pick's disease (33%), and hippocampal sclerosis (70%), as well as Huntington disease and argyrophilic grain disease in a small proportion of cases [7]. Based on cerebral immunohistochemistry, the pattern of TDP deposition in AD has been divided into six distinct topographic stages by Josephs *et al.* [8, 9]. Although the distribution of TDP-43 has been described in AD [9], FTLD [10], and ALS [11], its distribution pattern in PART is still unclear.

To address this issue, in the present study we analyzed the immunohistochemical results for pTDP-43 in 16 definite PART brains, using the phosphorylation-dependent anti-TDP-43 (pTDP-43, pS409/410) antibody, which specifically recognizes human TDP-43 phosphorylated at $pSer^{409}$ and $pSer^{410}$. TDP-43 is predominantly localized to the nucleus. Pathological TDP-43 forms abnormal inclusions in neuronal perikarya and neurites, indicating that the redistribution of TDP-43 to the cytoplasm is a pathogenic mechanism. By evaluating the distribution pattern of pTDP-43 in PART, we will be able to better elucidate the differences between PART and AD.

Materials and Methods

Materials

We investigated three independent groups (Table 1): 16 PART brains, 11 AD (Braak NFT stage ≥ IV and CERAD plaque density C) and pre-AD (Braak NFT stage III and CERAD plaque density C or B) cases, and 9 aging control cases (with neither NFTs nor Aβ). All cases were from our newly-established Brain Bank in the School of Medicine, Zhejiang University, China. The PART cases had undergone a detailed neuroanatomical examination, while the AD, pre-AD, and aging control cases had only been checked in the limbic areas, testing the difference in their distribution characteristics between PART and AD. This research was approved by the Medical Ethics Committee of Zhejiang University School of Medicine.

Immunohistochemistry

Immunohistochemistry was performed on formalin-fixed, paraffin-embedded tissues from autopsy cases. Small blocks of brain were dissected at autopsy and fixed in formalin in 0.1 mol/L phosphate buffer (pH 7.4) for 2 days. After cryoprotection in 15% sucrose in 0.01 mol/L phosphate-buffered saline (PBS, pH 7.4), the blocks were cut at 3 μm on a microtome (Leica, RM2235, Heidelberger, Germany). Free-floating sections were incubated with 3% H_2O_2 for 10 min to eliminate endogenous peroxidase activity. Before immunostaining, sections underwent microwave antigen retrieval for 15 min in citrate buffer (pH 6.0). After washing with PBS containing 0.3% Triton X-100 (Tx-PBS) for 30 min, sections were blocked in 10% normal serum, and then incubated with the primary antibody for 24 h in a cold room (4 °C). After treatment with the appropriate secondary antibody, labeling was detected using the avidin-biotinylated HRP complex (ABC) system (Vector Laboratories, Burlingame, CA). The peroxidase reaction was carried out using a developer solution containing 0.4 mg/mL DAB and 0.0006% hydrogen peroxide dissolved in TBS. For the negative control, the primary antibodies were omitted and all other steps were carried out as described above.

In AD, pre-AD, and aging control cases, the presence and severity of pTDP-43 immunoreactivity was assessed in the amygdala and hippocampus including the entorhinal cortex (EC). More extensive anatomical sampling was performed in the PART cases, allowing pTDP-43 pathology to be assessed in the amygdala, hippocampus, EC, temporal neocortex, frontal neocortex, parietal neocortex, occipital neocortex, putamen/pallidum/insular cortex (PPI),

Table 1 Demographics and pathology of all cases.

	PART	AD and pre-AD	Control
Number of cases	16	11	9
Mean age at death ± SD (years)	78.9 ± 7.2	83.8 ± 8.0	57.9 ± 6.9
Sex, M:F	12:4	6:5	6:3
Median Braak NFT stage	2.5	4	–
Brain weight ± SD (g)	1180.8 ± 110.8	1181.3 ± 68.3	1320.0 ± 145.4

PART: Braak NFT stage ≤ IV and Thal Aβ Phase 0; AD (7 cases): Braak NFT stage ≥ IV and CERAD SP density C; Pre-AD (4 cases): Braak NFT stage III and CERAD SP density C or B.

substantia nigra (SN), medulla oblongata (MO), and cerebellum. pTDP-43 pathology was semi-quantitatively scored based on a four-point scale: 0, no detectable pathology across the entire section; 1, slight (1–2 inclusions) or mild (< 5 inclusions in most fields at 100× magnification); 2, moderate (some pathology in most fields at 100× magnification); and 3, severe (much more pathology in most fields at 100× magnification). The reproducibility of the pTDP-43 pathological severity score (0–3) was checked by two independent researchers blind to case details. The primary antibodies used and their dilutions were: anti-tau AT8 (1:200; mouse monoclonal, Thermo Science, Rockford, IL), anti-amyloid β protein (1:200; mouse monoclonal, Sigma-Aldrich, St. Louis, MO), and anti-pTDP-43 (1:600; rabbit polyclonal, Sigma-Aldrich).

Fluorescent Double-Labeling

We used free-floating sections for double-labeling immunofluorescence of pTDP-43 and phosphorylated tau in PART and AD cases. The sections were incubated overnight at 4 °C with pTDP-43 and AT8 antibodies. After washing with Tx-PBS for 30 min, the sections were incubated overnight at room temperature in a cocktail of fluorescein isothiocyanate-conjugated goat anti-mouse IgG (1:250, AF488) and tetramethylrhodamine isothiocyanate-conjugated goat anti-rabbit IgG (1:500, Cy3). After washing, the sections were fixed in 2% paraformaldehyde for 15 min for protein protection, followed by washing in 1 × PBS for 30 min. To quench autofluorescence, the sections were immersed in Sudan Black B solution (0.3% SBB + 70% ethanol + 1 × PBS) at room temperature for 20 min. Then the sections were washed in a PBS solution with 0.02% Tween 20 and DAPI for 20 min, washed in PBS for another 5 min, and mounted on slides. They were then coverslipped with a fluorescence mounting medium (Vector Laboratories) and checked using a confocal laser microscope (Olympus FV-3000).

Data Analysis

Data were analyzed using SPSS software for Windows. For intra-group comparison of means, the Kruskal–Wallis test was used. Statistical associations between variables were measured using the Mann–Whitney test.

Results

Accumulation of Phosphorylated TDP-43 in PART

We used a phosphorylation-dependent anti-TDP-43 antibody for immunohistochemical staining of brains from 16 definite PART cases, 12 males and 4 females. Their Braak stages were ≤ IV and Thal Aβ Phase was 0, with no concurrent diseases associated with NFTs. The median age was 78.9 years ± 7.2 years (interquartile range, 60 years–98 years). The average brain weight was (1180.8 ± 110.8) g.

pTDP-43 staining showed a large variation in severity and regional distribution among PART cases (Table 2). pTDP-43 inclusions were found in the amygdala of all 16 PART cases, in the EC of 13, the subiculum of 10, the CA region (mainly CA1) of 10, and in the hippocampal dentate gyrus (DG) region of 3 cases. The number of inclusions varied among cases. In the cortical areas, pTDP-43 inclusions were found in the temporal cortex in 3 cases and in the parietal cortex in 2, but not in the frontal or occipital neocortex. In the subcortical and brainstem areas, positive pTDP-43 structures were found in the PPI in only 2 cases, but not in the MO or SN region. No pTDP-43-positive inclusions were found in the cerebellum of any of the cases (Fig. 1).

There was a correlation between the Braak NFT stage and pTDP-43 distribution in PART (Fig. 2). The density of pTDP-43 inclusions in PART was low in stage I–II cases, moderate in stage III cases, and high in stage IV cases with statistically significant differences in the means of their scores (Fig. 3A). Groups at different Braak NFT stages also showed statistically significant differences in the means of their scores for both the hippocampus (Fig. 3B) and the amygdala (Fig. 3C). In PART cases at stages I–III, pTDP-43-positive neuronal cytoplasmic inclusions (NCIs) were present in the amygdala and the hippocampus to various extents, but not in the DG region. The pTDP-43 immunoreactivity was only noted in the DG region of three PART cases at stage IV, and the density was very low (Fig. 2D). pTDP-43-positive NCIs were observed in the neocortex, mild in the temporal and parietal cortex, but absent in the frontal and occipital cortex. We found a low density of pTDP-43-positive NCIs in the PPI in PART cases at stage IV, but they were absent in the SN and MO. There were statistically significant differences in the means of the pTDP-43 scores between the amygdala and the temporal cortex/PPI, as well as between the EC and the temporal cortex/PPI (Fig. 3D).

In summary, we identified four stages indicative of potentially sequential dissemination of pTDP-43 in PART: stage I involved the amygdala, stage II the hippocampus; stage III the neocortex, and stage IV the subcortical PPI (Fig. 4).

Table 2 pTDP-43-positive structures in PART cases.

Case	Age	Sex	NFT (Braak)	Amyg	EC	Sub	CA	DG	T	F	P	O	PPI	SN	MO	C
1	60	M	I	1	1	1	1	–	–	–	–	–	–	–	–	–
2	74	F	I	1	1	1	1	–	–	–	–	–	–	–	–	–
3	76	M	I	1	–	–	–	–	–	–	–	–	–	–	–	–
4	80	M	I	1	–	–	–	–	–	–	–	–	–	–	–	–
5	84	M	I	1	1	1	1	–	–	–	–	–	–	–	–	–
6	91	M	I	1	1	–	–	–	–	–	–	–	–	–	–	–
7	65	F	II	1	1	–	–	–	–	–	–	–	–	–	–	–
8	77	M	II	1	1	–	–	–	–	–	–	–	–	–	–	–
9	83	M	II	1	–	–	–	–	–	–	–	–	–	–	–	–
10	80	F	III	3	3	3	2	–	1	–	2	–	1	–	–	–
11	81	F	III	2	2	1	1	–	–	–	–	–	–	–	–	–
12	83	F	III	1	2	2	2	–	1	–	–	–	–	–	–	–
13	74	M	IV	3	3	3	3	1	–	–	–	–	–	–	–	–
14	78	M	IV	2	2	2	1	1	–	–	–	–	–	–	–	–
15	79	M	IV	3	2	2	1	–	–	–	–	–	–	–	–	–
16	98	M	IV	3	3	3	3	1	1	–	1	–	1	–	–	–

NFT, neurofibrillary tangle; Amyg, amygdala; EC, entorhinal cortex; Sub, subiculum; CA, cornu ammonis; DG, dentate gyrus; T, temporal cortex; F, frontal cortex; P, parietal cortex; O, occipital cortex; PPI, putamen/pallidum/insular cortex; SN, substantia nigra; MO, medulla oblongata; C, cerebellum.

–, None; 1, slight/mild; 2, moderate; 3, severe.

Accumulation of Phosphorylated TDP-43 in AD and Pre-AD

It has been reported that TDP-43 is present in AD and the aging human brain [12, 13]. Since pTDP-43 inclusions in our PART cases tended to be more restricted to the limbic system, we selected 11 AD and pre-AD and 9 aging control cases from our brain bank to compare the pTDP-43 distribution in the above regions. The mean age of the AD and pre-AD cases was 84.2 years ± 7.4 years, with an average brain weight of 1157.3 g ± 71.8 g. The mean age of the control cases was 57.1 years ± 6.8 years, with an average brain weight of 1293.0 g ± 146.9 g. pTDP-43 inclusions were found in all AD and pre-AD cases (11/11) with variations in frequency and regional distribution (Table 3). No pTDP-43-positive inclusions were found in any of the control cases (Table S1).

In the limbic region of the 11 AD and pre-AD cases, the density of pTDP-43 inclusions was low in those at Braak stage III, moderate at stage IV, and high at stage VI (Fig. 5). The pTDP-43 pathology in the DG of AD cases was more severe than that of PART cases. In PART cases, no pTDP-43 pathology was found in the DG in cases with NFT Braak stages I–III, and it was very sporadic in cases at stage IV. Compared to the PART cases, pTDP-43 pathology in the DG was evident in pre-AD cases at stage III, severe in AD cases at stage IV, and more severe in AD cases at stage VI (Fig. 5).

Two major types of pTDP-43 pathology were found in the PART, AD and pre-AD cases. They were characterized predominantly either by long aggregates in dendrites (neuritic type), or by perikaryal pTDP-43 inclusions (cytoplasmic type). Fluorescence double-labeling showed that tau-positive neuropil threads and pTDP-43-positive dystrophic neurites were co-stained in the hippocampus, some neurons showing neuritic-type immunoreactivity for both markers (Fig. 6).

Discussion

Here, we found that pTDP-43 expression in PART cases could be classified into 4 stages, indicative of the sequential involvement of brain regions. This finding differs from the report on FTLD describing four patterns of pTDP-43 [10]. In that report, pattern I was characterized by pTDP-43 lesions in the orbital gyrus, gyrus rectus, and amygdala; pattern II showed pTDP-43 lesions in the middle frontal, anterior cingulate gyrus and anteromedial temporal lobe, the superior and medial temporal gyri, striatum, red nucleus, thalamus, and pre-cerebellar nuclei; pattern III involved the motor cortex, bulbar somatomotor neurons, and the anterior horn of the spinal cord; and pattern IV was characterized by pTDP-43 lesions in the visual cortex. In ALS, four stages of pTDP-43 pathology have also been reported—stage 1 with lesions in the

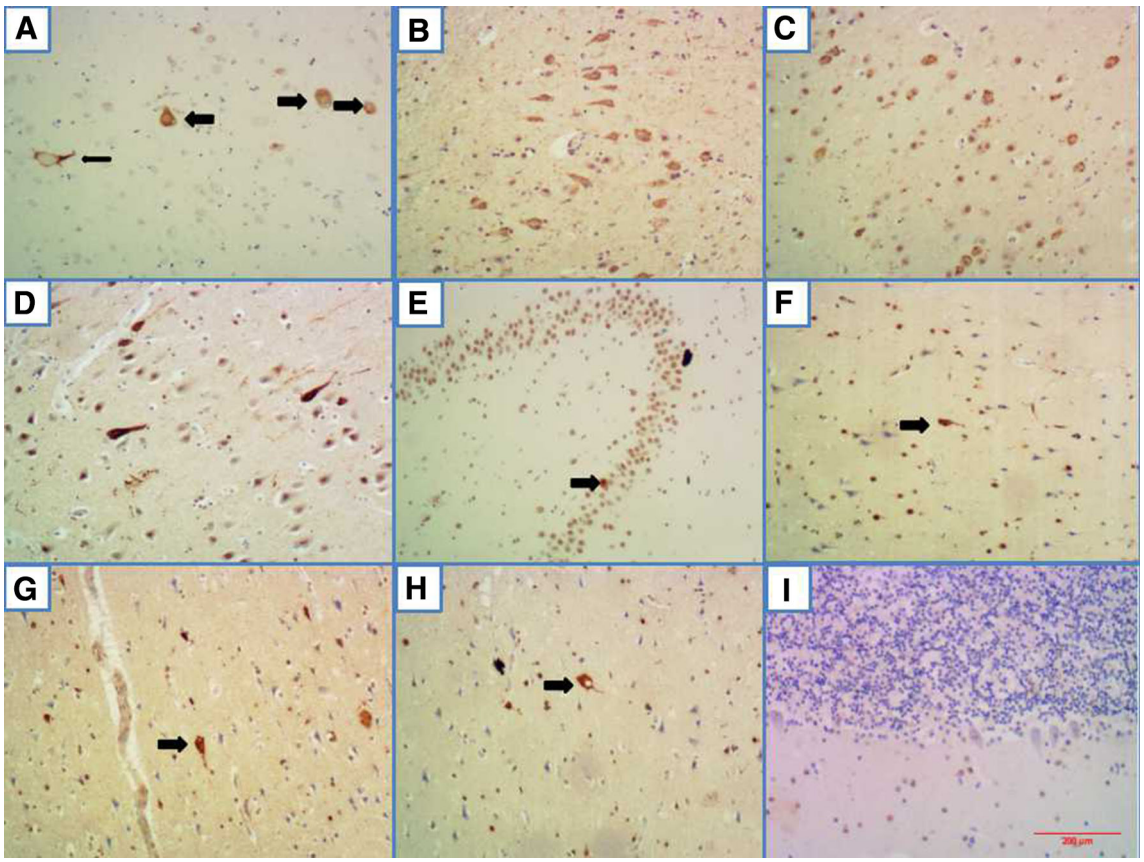

Fig. 1 Phosphorylated TDP-43 pathology in PART cases. **A** Neuronal cytoplasmic inclusions (NCIs) (thick arrows) and a dystrophic neurite (DN) (thin arrow) in the amygdala. **B** Neurofibrillary tangle-like structures in the entorhinal cortex. **C** Small round NCIs in the subiculum. **D** Neurofibrillary tangle-like structures in the pyramidal layer of the CA1 region. **E** One NCI in a granule cell in the dentate gyrus. **F** A neurofibrillary tangle-like structure (arrow) in the temporal cortex. **G** A neurofibrillary tangle-like structure (arrow) in the parietal cortex. **H** A neurofibrillary tangle-like structure (arrow) in the PPI. **I** No positive pTDP-43 structures in the cerebellum. Scale bar, 200 μm.

agranular motor cortex, brainstem motor nuclei, and spinal motoneurons; stage 2 with involvement of the prefrontal neocortex, brainstem reticular formation, pre-cerebellar nuclei, and red nucleus; stage 3 involved the prefrontal and postcentral neocortex and striatum; and stage 4 showed pTDP-43 inclusions in anteromedial portions of the temporal lobe, including the hippocampus [11]. This pattern also differs from our findings in PART cases.

Intracellular accumulation of TDP-43 has been reported in patients with dementia other than FTLD and ALS, including AD. Regarding the distribution of TDP-43 pathology in AD, Amador-Ortiz *et al.* first classified it into limbic and diffuse types, and indicated that limbic involvement was more common [14]. Subsequently, TDP-43 pathology in AD was found to spread from limbic structures to association cortices [15]. Recently, Josephs *et al.* suggested a six-level TDP-43 staging scheme for AD, which starts from the amygdala (stage I), to the EC and subiculum (stage II), to the DG of the hippocampus and occipitotemporal cortex (stage III), to the insular cortex, ventral striatum, basal forebrain, and inferior temporal cortex (stage IV), to the SN, inferior olive, and midbrain tectum (stage V), and finally to the basal ganglia and middle frontal cortex (stage VI) [9]. However, the pathological pattern of TDP-43 expression in PART cases was still unknown. To address this issue, we performed immunohistochemical analysis using a phosphorylation-dependent anti-TDP-43 antibody in the above areas of our PART cases. Furthermore, pTDP-43 pathology in the limbic system was compared between PART and AD cases.

We found a high frequency of pTDP-43 pathology in the PART cases, among whom there appeared to be a hierarchy in its anatomical distribution and severity. This suggests a progressive evolution of PART, with pTDP-43 expression spreading from the amygdala to other limbic structures first, and then to the association cortices, and finally to the PPI. Based on our findings on the anatomical location of pTDP-43 expression and the density (severity scores) of pTDP-43-positive cells in the PART brain, it is possible

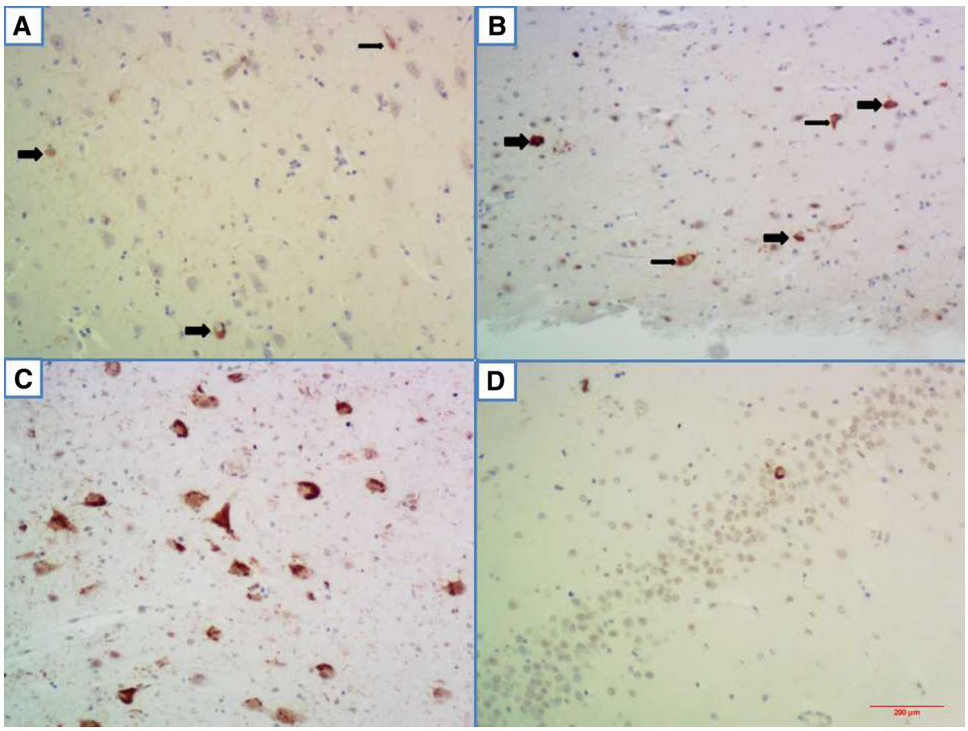

Fig. 2 Phosphorylated TDP-43-positive structures in PART cases at different Braak stages. **A** A few neuronal cytoplasmic inclusions (NCIs) (thick arrows) and dystrophic neurites (DNs) (thin arrow) in the amygdala of a PART case at Braak stage I. **B** Moderate NCIs (thick arrows) and DNs (thin arrows) in the amygdala of a PART case at Braak stage III. **C** Massive NCIs and DNs in the hippocampus of a PART case at Braak stage IV. **D** One NCI in a granule cell of the dentate gyrus of a PART case at Braak stage IV. All images are at 100× magnification. Scale bar, 200 μm.

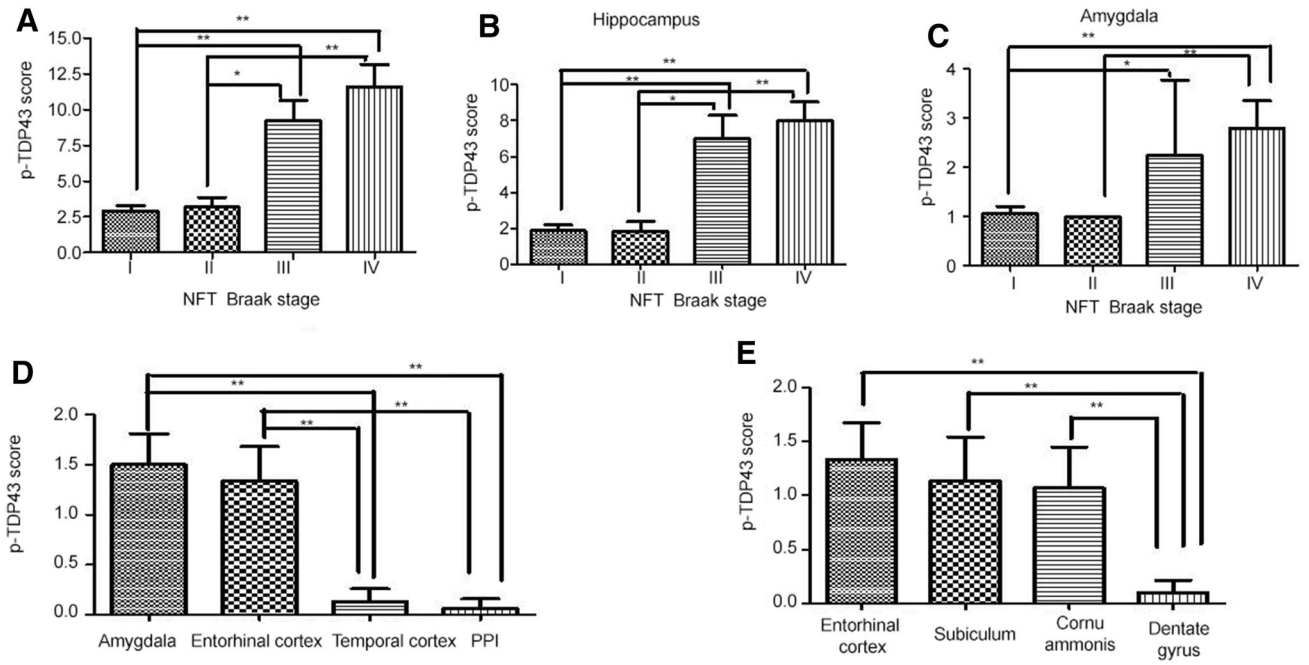

Fig. 3 Correlation between Braak stages and pTDP-43 density scores in PART cases. **A**–**C** Mean pTDP-43 pathology scores in PART cases at four Braak stages (**A**), in the hippocampus (**B**), and in the amygdala (**C**) (*$P < 0.05$; **$P < 0.01$). **D**, **E** Mean pTDP-43 scores in the amygdala, EC, temporal cortex, and PPI (**D**), and in the hippocampal region (EC, subiculum, CA, and DG) (**E**) (**$P < 0.01$).

that there is a spatial sequence of pTDP-43 pathology dissemination with the amygdala involved first, followed by the EC and subiculum, then the CA and DG (Fig. 3D, E).

Although the amygdala is the starting-point for both PART and AD, the evolving pattern in PART cases differs from that in AD based on our findings and the reported TDP-43 staging scheme of AD. First, pTDP-43 stage II of PART involved the entorhinal, subiculum, and CA regions

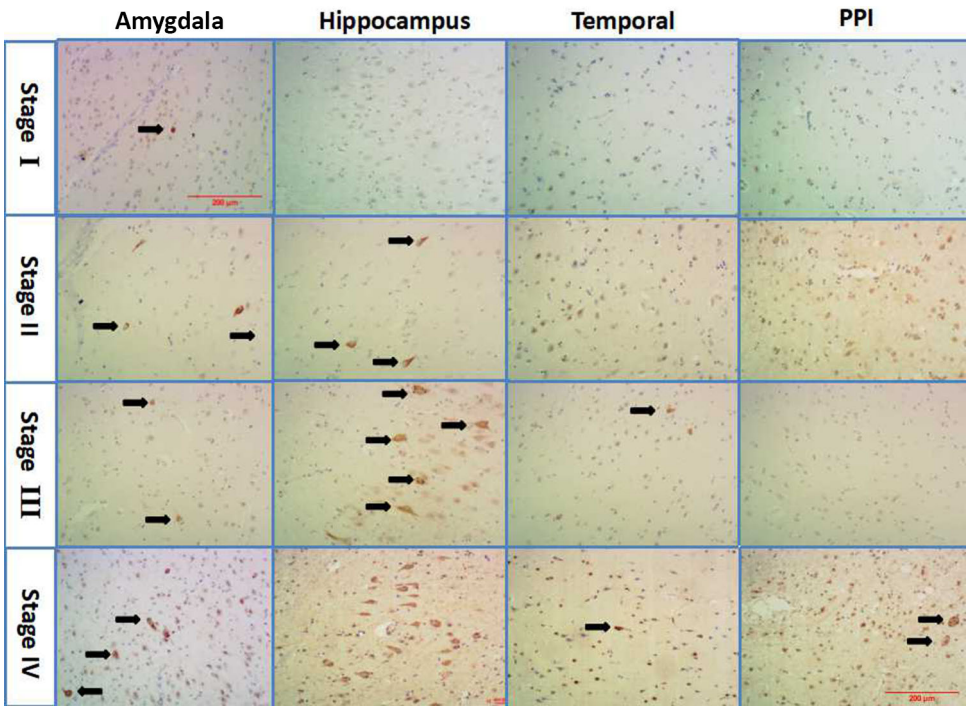

Fig. 4 Pathology of PART from representative cases at four stages. Stage I, scant-sparse pTDP-43 immunoreactive inclusions are present only in the amygdala. Stage II, moderate-frequent inclusions are present in the amygdala and the entorhinal cortex, but not in the dentate gyrus and the temporal cortex. Stage III, inclusions spread to the temporal and parietal cortices. Stage IV, inclusions spread to the PPI. The pathology starts from the amygdala and then progresses to other limbic structures before involving the neocortex and PPI. Among the neocortical regions, the temporal and parietal lobes were less frequently involved, while the frontal and occipital lobes were not affected in our PART cases. Arrows indicate NCIs. Scale bars, 200 μm.

Table 3 pTDP-43-positive structures in AD and pre-AD cases.

Case no.	Age	Sex	SP (CERAD)	NFT (Braak)	Amyg	EC	Sub	CA	DG
1	93	F	B	III	–	2	1	–	–
2	69	F	C	III	1	1	1	1	1
3	79	F	C	III	–	1	1	1	–
4	90	M	C	III	1	1	1	–	–
5	78	M	C	IV	1	1	–	–	–
6	81	F	C	IV	3	2	1	1	2
7	83	M	C	IV	1	1	1	1	–
8	98	F	C	IV	2	2	–	–	–
9	79	M	C	VI	1	2	2	1	–
10	85	M	C	VI	3	3	3	3	1
11	88	F	C	VI	3	3	3	3	2

AD, Braak NFT stage ≥ IV and CERAD SP density C; Pre-AD, Braak NFT stage III and CERAD SP density C or B; SP, senile plaque; NFT, neurofibrillary tangle; Amyg, amygdala; EC, entorhinal cortex; Sub, subiculum; CA, cornu ammonis; DG, dentate gyrus.

–, None; 1, mild/slight; 2, moderate; 3, severe.

(mainly CA1), but did not involve the DG. No pTDP-43 was found in the pyramidal cell layer of the DG in any of our PART cases at Braak stages I–III. Only 3 PART cases at Braak stage IV showed very few pTDP-43 NCIs in the pyramidal cell layer of the DG, which differs from reports in AD and our findings in the AD as well as the pre-AD cases. Second, PART cases at pTDP-43 stage III showed a low density of pTDP-43 NCIs in the temporal and parietal neocortex, but not in the frontal and occipital cortex. Third, PART cases at pTDP-43 stage IV showed sporadic pTDP-43 pathology in the PPI areas. No pTDP-43 pathology was found in the midbrain (SN and MO) and the middle frontal

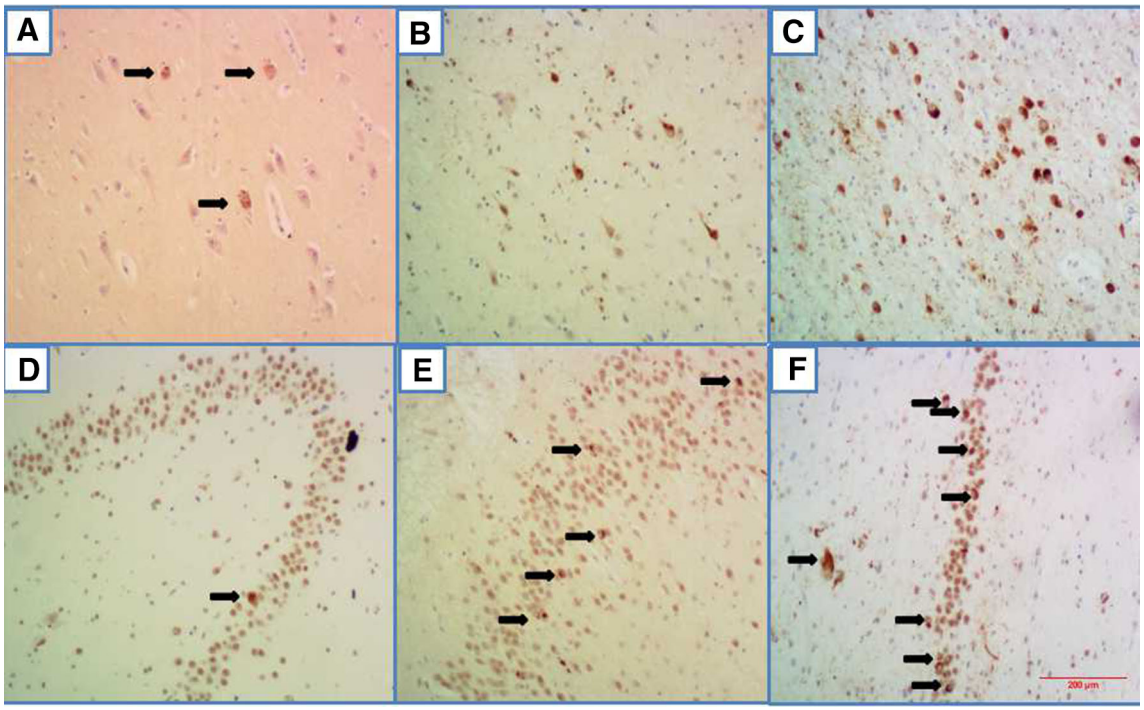

Fig. 5 Phosphorylated TDP-43-positive structures in the limbic system of AD and PART cases at different Braak stages. **A** A few NCIs (arrows) in the amygdala of an pre-AD case at stage III. **B** Some neurofibrillary tangle-like structures in the amygdala of an AD case at stage IV. **C** Massive NCIs and dystrophic neurites (DNs) in the hippocampus of an AD case at stage VI. **D** One NCI in a granule cell of the dentate gyrus of a PART case at stage IV. **E** Some NCIs in the dentate granule cells of an AD case at stage IV. **F** Massive NCIs in granule cells of the dentate gyrus of an AD case at stage VI. Scale bar, 200 μm.

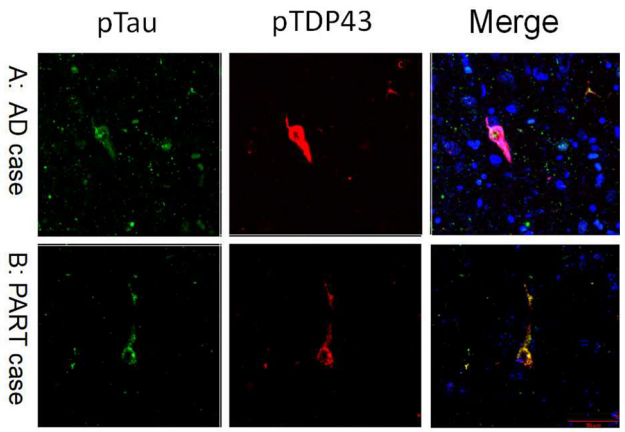

Fig. 6 Double-labeling immunofluorescence images for tau tangles and pTDP-43 pathology in pyramidal neurons of the hippocampal CA region. Representative images of tau and pTDP-43 staining in an AD case (**A**) and a PART case (**B**). Tau-positive neuropil threads (green) and pTDP-43-positive DNs (red) in pyramidal cells of the CA region are co-localized; there is also co-localization of tau and pTDP-43 in some neuronal cytoplasmic inclusions. Scale bar, 50 μm.

cortex in our cases. In general, PART mainly affected the limbic system.

We found that pTDP-43 pathology was present in the amygdala and other limbic structures in all AD and pre-AD cases (11/11, 100%), but negative in all aging control cases (0/9). Since the case selection procedure and the anatomical regions evaluated were not the same as those of previous reports, it is to be expected that the incidence of pTDP-43 differs from that of those studies [16–18]. There was also a correlation between the NFT Braak stage and pTDP-43 density: the higher the Braak stage, the more severe the pTDP-43 pathology, especially the pTDP-43 density in the granule cell layer of the DG. The DG pTDP-43 pathology was evident in pre-AD cases at Braak stage III and was more severe in AD at Braak stage VI. In our PART cases, the density of DG pTDP-43 NCIs was very low in Braak stage IV and negative in all Braak stage I–III cases. DG pathology is an indicator of memory impairment. The discrete patterns of pTDP-43 pathology in the DG of PART and AD cases may reflect difference in their clinical manifestations. Based on this finding, we hypothesize that a difference in the density of pTDP-43 NCIs in the DG is one of the key parameters that differentiate PART from AD, and may also reflect differences in their clinical manifestations [19–21]. Furthermore, the majority of the pTDP-43 pathology observed in PART cases was similar to tau morphology. They displayed tangle-like, short thread-like or coiled body-like structures. Fluorescent double labeling showed that at least a subset of TDP-43-positive neurites manifested with tau pathology in the same

neurons, suggesting that the TDP-43 pathology found in this study may be related to PART pathology in some way [22].

The present study is the first to elucidate a relationship between pTDP-43 pathology and the phenotypes of PART. First of all, pTDP-43 expression in various brain areas suggests that pTDP-43 pathology is common in the PART brain. Second, the distribution of pTDP-43 pathology in our PART cases is similar to that reported in AD, but tends to be more restricted to the limbic system. The pTDP-43 pathology in PART differs to some extent from that in AD, especially in the DG. Furthermore, the evolving pattern of pTDP-43 pathology in the limbic system in PART suggests that there might be a process leading to pTDP-43 dissemination from the EC to the DG. Finally, the co-existence of abnormal deposition of pTDP-43 and phosphorylated tau in PART was discernible. Since the pattern of pTDP-43 pathology in PART is similar to that reported in AD with low TDP-43 stages, it might be possible that pTDP-43 pathology contributes to both neurodegenerative diseases [23]. Further studies using larger cohorts with more detailed clinical and pathological data are needed to elucidate the clinical impact of pTDP-43 pathology in PART [24–27].

Acknowledgements We thank the families of the patients who donated their brains to China Brain Bank in Zhejiang University School of Medicine and allowed the completion of this study. This work was supported by the National Science Foundation China (91632109 to JHZ, KQZ and HJH), the Zhejiang Provincial Natural Science Foundation (LY16H090013 to KQZ), and the Zhejiang Medical and Health Science and Technology Plan Project (WKJ2013-2-009 to KQZ).

Compliance with Ethical Standards

Conflict of interest The authors declare that there is no conflict of interest.

References

1. Crary JF, Trojanowski JQ, Schneider JA, Abisambra JF, Abner EL, Alafuzoff I, *et al.* Primary age-related tauopathy (PART): a common pathology associated with human aging. Acta Neuropathol 2014, 128: 755–766.
2. Duyckaerts C, Braak H, Brion JP, Buée L, Del Tredici K, Goedert M, *et al.* PART is part of Alzheimer disease. Acta Neuropathol 2015, 129: 749–756.
3. Jellinger KA, Alafuzoff I, Attems J, Beach TG, Cairns NJ, Crary JF, *et al.* PART, a distinct tauopathy, different from classical sporadic Alzheimer disease. Acta Neuropathol 2015, 129: 757–762.
4. Neumann M, Sampathu DM, Kwong LK, Truax AC, Micsenyi MC, Chou TT, *et al.* Ubiquitinated TDP-43 in frontotemporal lobar degeneration and amyotrophic lateral sclerosis. Science 2006, 314: 130–133.
5. Cykowski MD, Powell SZ, Peterson LE, Appel JW, Rivera AL, Takei H, *et al.* Clinical significance of TDP-43 neuropathology in amyotrophic lateral sclerosis. J Neuropathol Exp Neurol 2017, 76: 402–413.
6. Hasegawa M, Arai T, Nonaka T, Kametani F, Yoshida M, Hashizume Y, *et al.* Phosphorylated TDP-43 in frontotemporal lobar degeneration and amyotrophic lateral sclerosis. Ann Neurol 2008, 64: 60–70.
7. Warraich ST, Yang S, Nicholson GA, Blair IP. TDP-43: a DNA and RNA binding protein with roles in neurodegenerative diseases. Int J Biochem Cell Biol 2010, 42: 1606–1609.
8. Josephs KA, Murray ME, Whitwell JL, Parisi JE, Petrucelli L, Jack CR, *et al.* Staging TDP-43 pathology in Alzheimer's disease. Acta Neuropathol 2014, 127: 441–450.
9. Josephs KA, Murray ME, Whitwell JL, Tosakulwong N, Weigand SD, Petrucelli L, *et al.* Updated TDP-43 in Alzheimer's disease staging scheme. Acta Neuropathol 2016, 131: 571–585.
10. Brettschneider J, Del Tredici K, Irwin DJ, Grossman M, Robinson JL, Toledo JB, *et al.* Sequential distribution of pTDP-43 pathology in behavioral variant frontotemporal dementia (bvFTD). Acta Neuropathol 2014, 127: 423–439.
11. Brettschneider J, Del Tredici K, Toledo JB, Robinson JL, Irwin DJ, Grossman M, *et al.* Stages of pTDP-43 pathology in amyotrophic lateral sclerosis. Ann Neurol 2013, 74: 20–38.
12. Arai T, Mackenzie IR, Hasegawa M, Nonoka T, Niizato K, Tsuchiya K, *et al.* Phosphorylated TDP-43 in Alzheimer's disease and dementia with Lewy bodies. Acta Neuropathol 2009, 117: 125–136.
13. Uchino A, Takao M, Hatsuta H, Sumikura H, Nakano Y, Nogami A, *et al.* Incidence and extent of TDP-43 accumulation in aging human brain. Acta Neuropathol Commun 2015, 3: 35.
14. Amador-Ortiz C, Lin WL, Ahmed Z, Personett D, Davies P, Duara R, *et al.* TDP-43 immunoreactivity in hippocampal sclerosis and Alzheimer's disease. Ann Neurol 2007, 61: 435–445.
15. Hu WT, Josephs KA, Knopman DS, Boeve BF, Dickson DW, Petersen RC, *et al.* Temporal lobar predominance of TDP-43 neuronal cytoplasmic inclusions in Alzheimer disease. Acta Neuropathol 2008, 116: 215–220.
16. Nascimento C, Suemoto CK, Rodriguez RD, Alho AT, Leite RP, Farfel JM, *et al.* Higher prevalence of TDP-43 proteinopathy in cognitively normal Asians: a clinicopathological study on a multiethnic sample. Brain Pathol 2016, 26: 177–185.
17. Wilson AC, Dugger BN, Dickson DW, Wang DS. TDP-43 in aging and Alzheimer's disease - a review. Int J Clin Exp Pathol 2011, 4: 147–155.
18. Geser F, Robinson JL, Malunda JA, Xie SX, Clark CM, Kwong LK, *et al.* Pathological 43-kDa transactivation response DNA-binding protein in older adults with and without severe mental illness. Arch Neurol 2010, 67: 1238–1250.
19. Josephs KA, Whitwell JL, Weigand SD, Murray ME, Tosakulwong N, Liesinger AM, *et al.* TDP-43 is a key player in the clinical features associated with Alzheimer's disease. Acta Neuropathol 2014, 127: 811–824.
20. Davidson YS, Raby S, Foulds PG, Robinson A, Thompson JC, Sikkink S, *et al.* TDP-43 pathological changes in early onset familial and sporadic Alzheimer's disease, late onset Alzheimer's disease and Down's syndrome: association with age, hippocampal sclerosis and clinical phenotype. Acta Neuropathol 2011, 122: 703–713.
21. Josephs KA, Murray ME, Tosakulwong N, Whitwell JL, Knopman DS, Machulda MM, *et al.* Tau aggregation influences cognition and hippocampal atrophy in the absence of beta-amyloid: a clinico-imaging-pathological study of primary age-related tauopathy (PART). Acta Neuropathol 2017, 133: 705–715.

22. Smith VD, Bachstetter AD, Ighodaro E, Roberts K, Abner EL, Fardo DW, *et al.* Overlapping but distinct TDP-43 and tau pathologic patterns in aged hippocampi. Brain Pathol 2018, 28: 264–273.
23. Chang XL, Tan MS, Tan L, Yu JT. The role of TDP-43 in Alzheimer's disease. Mol Neurobiol 2016; 53: 3349–3359.
24. Arnold SJ, Dugger BN, Beach TG. TDP-43 deposition in prospectively followed, cognitively normal elderly individuals: correlation with argyrophilic grains but not other concomitant pathologies. Acta Neuropathol 2013, 126: 51–57.
25. McAleese KE, Walker L, Erskine D, Thomas AJ, McKeith IG, Attems J. TDP-43 pathology in Alzheimer's disease, dementia with Lewy bodies and ageing. Brain Pathol 2017, 27: 472–479.
26. Wang QH, Wang X, Bu XL, Lian Y, Xiang Y, Luo HB, *et al.* Comorbidity burden of dementia: A hospital-based retrospective study from 2003 to 2012 in seven cities in China. Neurosci Bull 2017, 33: 703–710.
27. Nag S, Yu L, Wilson RS, Chen EY, Bennett DA, Schneider JA. TDP-43 pathology and memory impairment in elders without pathologic diagnoses of AD or FTLD. Neurology 2017, 88: 653–660.